DOI: 10.1002/cbdv.201900370



CHEMISTRY & BIODIVERSITY

# Design, Synthesis, Molecular Docking, and Cholinesterase Inhibitory Potential of Phthalimide-Dithiocarbamate Hybrids as New Agents for Treatment of Alzheimer's Disease

Mehdi Asadi,[a] Mostafa Ebrahimi,[a] Maryam Mohammadi-Khanaposhtani,[b] Homa Azizian,[c] Saghi Sepehri,[d] Hamid Nadri,[e] Mahmood Biglar,[f] Massoud Amanlou,[a] Bagher Larijani,[f] Roghieh Mirzazadeh,*[g] Najmeh Edraki,[h] and Mohammad Mahdavi*[f]

[a] Department of Medicinal Chemistry, Faculty of Pharmacy and Pharmaceutical Sciences Research Center, Tehran University of Medical Sciences, 1417653761 Tehran, Iran

[b] Cellular and Molecular Biology Research Center, Health Research Institute, Babol University of Medical Sciences, Babol 4717647745, Iran

[c] Department of Medicinal Chemistry, School of Pharmacy-International Campus, Iran University of Medical Sciences, Tehran 14665354 Iran

[d] Department of Medicinal Chemistry, School of Pharmacy, Ardabil University of Medical Sciences, Ardabil 5618953141, Iran

[e] Department of Medicinal Chemistry, Faculty of Pharmacy and Pharmaceutical Sciences Research Center, Shahid Sadoughi University of Medical Sciences, Yazd 8915173160, Iran

[f] Endocrinology and Metabolism Research Center, Endocrinology and Metabolism Clinical Sciences Institute, Tehran University of Medical Sciences, Tehran 1417653761, Iran,, e-mail: momahdavi@tums.ac.ir

[g] Department of Biochemistry, Pasteur Institute of Iran, Tehran 1316943551, Iran,, e-mail: rmirzazadeh@pasteur.ac.ir

[h] Medicinal and Natural Products Chemistry Research Center, Shiraz University of Medical Sciences, Shiraz 7134853734, Iran

A novel series of phthalimide-dithiocarbamate hybrids was synthesized and evaluated for *in vitro* inhibitory potentials against acetylcholinesterase (AChE) and butyrylcholinesterase (BuChE). The anti-cholinesterase results indicated that among the synthesized compounds, the compounds **7g** and **7h** showed the most potent anti-AChE and anti-BuChE activities, respectively. Molecular docking and dynamic studies of the compounds **7g** and **7h**, respectively, in the active site of AChE and BuChE revealed that these compounds as well interacted with studied cholinesterases. These compounds also possessed drug-like properties and were able to cross the BBB.

**Keywords:** phthalimide, dithiocarbamate, Alzheimer's disease, acetylcholinesterase, butyrylcholinesterase, inhibitory activity.

## Introduction

Alzheimer's disease (AD) is a complex and age-related neurodegenerative progressive and fatal disorder.[1] It is estimated that people suffering dementia in 2018 were 50 million worldwide and this statistic is in progression.[2] Despite many efforts of pharmaceutical companies and academic institutions, there is no effective treatment for Alzheimer's disease. Therefore, the discovery of new efficient agents for the treatment of AD is a big challenge for the healthcare community.

Alzheimer's disease is characterized by shortage of neurotransmitter acetylcholine (ACh), accumulation of amyloid plaques, and tau-phosphorylation in the brain.[3] Therefore, increase of the level of ACh, decomposition of amyloid plaques, and inhibition of

Supporting information for this article is available on the WWW under https://doi.org/10.1002/cbdv.201900370

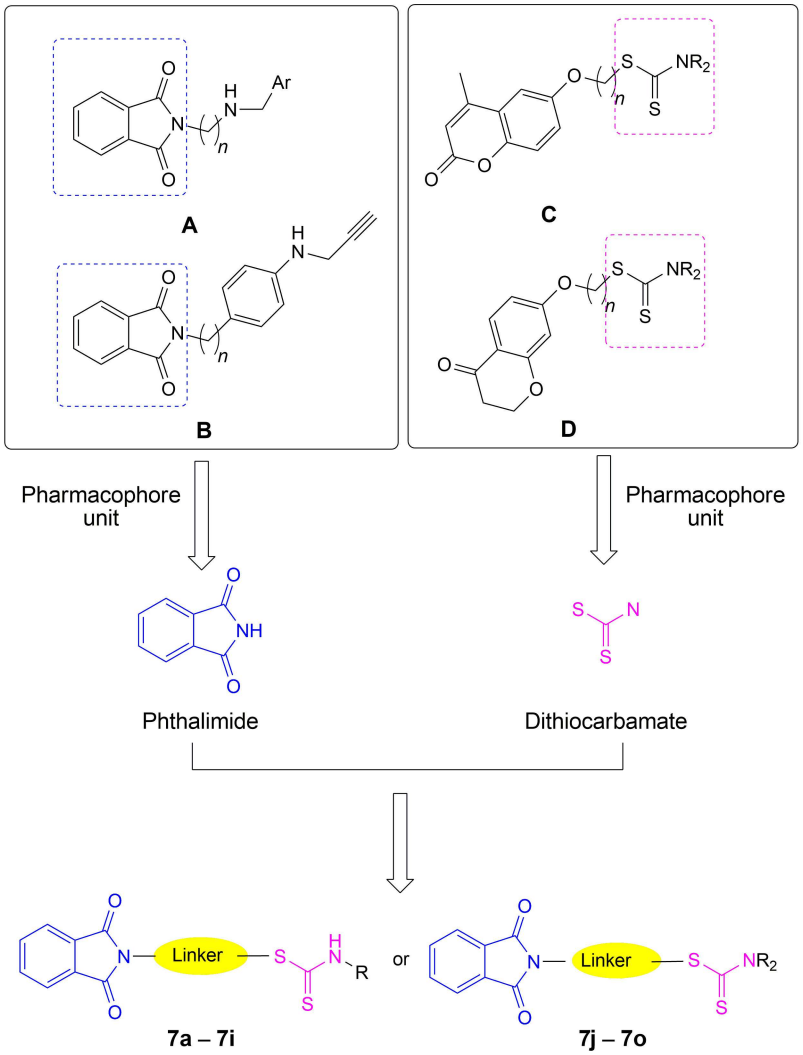


**Figure 1.** Design strategy of novel phthalimide-dithiocarbamate hybrids **7** as new anti-Alzheimer agent.

tau-phosphorylation and aggregation in the brain are the most important therapeutic targets for AD. Furthermore, several studies have suggested that increase levels brain derived neurotrophic factor (BDNF) and nerve growth factor (NGF) by experimental drugs such as J147 can be useful for treatment of AD.[4] The activity of acetylcholine in the brain is terminated by acetylcholinesterase (AChE) and therefore inhibition of this enzyme led to ameliorate signs and symptoms of AD.[5] Today, AChE inhibitors such as donepezil and rivastigmine are the main drugs for the treatment of AD.[6]

Another one of ACh degrading enzymes is butyrylcholinesterase (BuChE). Recent studies showed that activity of BuChE in the brain of AD patients with the progression of the AD increased while AChE activity in these patients declines. Therefore, inhibition of both types of ACh degrading enzymes may be beneficial in AD treatment.[7]

The phthalimide is a bicyclic heterocyclic scaffold and its derivatives have diverse range of biologically activities such as anti-inflammatory, anticonvulsant, hypolipidemic, analgesic, and immunomodulatory activities.[8–13] Recently, several derivatives of phthalimide with high inhibitory activity against AChE have been reported (*Figure 1A* and *B*).[14,15] On the other hand, two dithiocarbamate derivatives **C** and **D** exhibited good inhibitory activity against cholinesterases (*Figure 1*).[16,17] Keeping in view of the above mentioned importance of phthalimide and dithiocarbamate pharmacophores, herein, we designed, synthesized, and evaluated a novel series of phthalimide-dithiocarbamate hybrids as new anti-cholinesterase agents (*Figure 1*, compounds **7a**–**7i** and **7j**–**7o**).

 

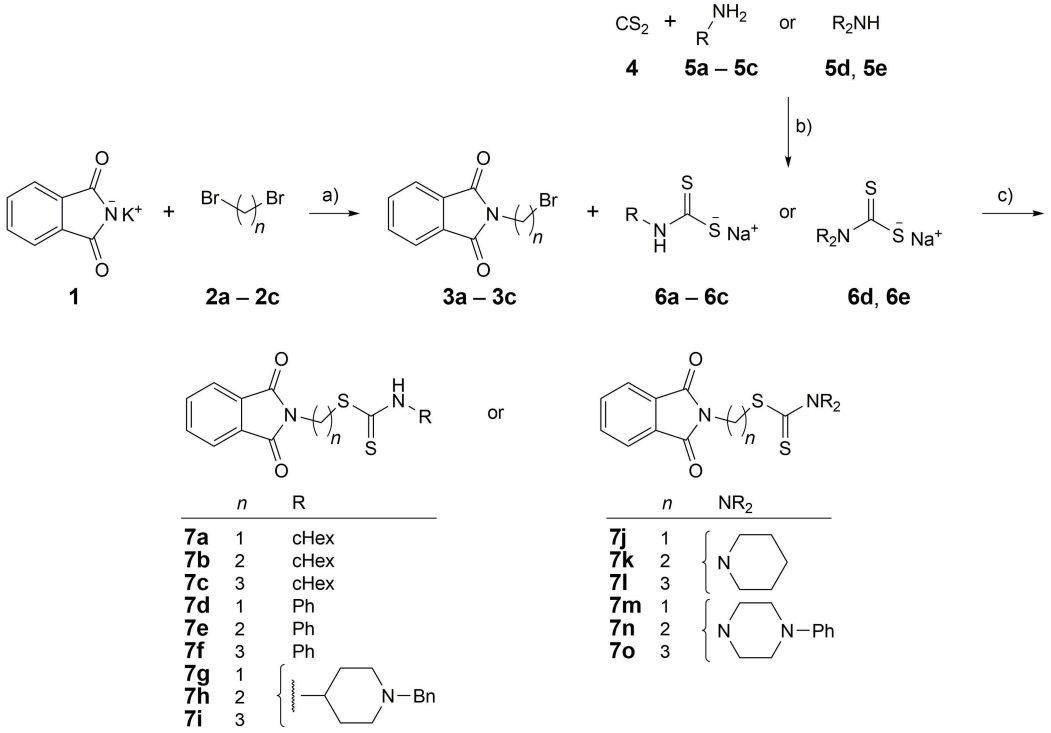


**Scheme 1.** Synthesis of phthalimide containing dithiocarbamate derivatives **7a**–**7o**. Reagents and conditions: a) Acetonitrile, 60 °C, 6 h; b) Potassium hydroxide 10%, DMF, 50 °C, 3 h; c) DMF, 50 °C, 12 h.

**Table 1.** Anti-ChE activities of compounds **7a**–**7o**.

| Compound | $IC_{50}$ [μM] (AChE)[a] | $IC_{50}$ [μM] (BuChE)[a] |
|---|---|---|
| **7a** | ≥100 | ≥100 |
| **7b** | 27.28 ± 0.61 | 11.7 ± 0.41 |
| **7c** | ≥100 | 14.95 ± 0.52 |
| **7d** | ≥100 | ≥100 |
| **7e** | ≥100 | 23.36 ± 0.59 |
| **7f** | ≥100 | ≥100 |
| **7g** | 4.6 ± 0.18 | 20.37 ± 0.37 |
| **7h** | 11.72 ± 0.21 | 8.8 ± 0.24 |
| **7i** | 28.25 ± 0.29 | ≥100 |
| **7j** | ≥100 | 20.6 ± 0.33 |
| **7k** | ≥100 | ≥100 |
| **7 l** | ≥100 | 30 ± 0.46 |
| **7m** | ≥100 | ≥100 |
| **7n** | ≥100 | ≥100 |
| **7o** | ≥100 | 13.6 ± 0.36 |
| Donepezil | 0.027 ± 0.003 | 7.79 ± 0.06 |
| Rivastigmine | 11.07 ± 0.01 | 7.72 ± 0.02 |

[a] Data are expressed as Mean ± SE (three independent experiments).

## Results and Discussion

### *Chemistry*

The general procedure for the synthesis of phthalimide containing dithiocarbamate derivatives **7a**–**7o** is presented in *Scheme 1*. It was started from the reaction of potassium 1,3-dioxoisoindolin-2-ide **1** and appropriate dibromoalkanes **2a**–**2c** in acetonitrile at 60 °C to give 2-(bromoalkyl)isoindoline-1,3-dione derivatives **3a**–**3c**. On the other hand, carbon disulfide (**4**) and primary amines **5a**–**5c** or secondary amines **5d**–**5e** reacted in presence of 10% potassium hydroxide in DMF at 50 °C to produce various sodium dithiocarbamate derivatives **6a**–**6e**. Finally, title compounds **7a**–**7o** were obtained from the reaction of 2-(bromoalkyl)isoindoline-1,3-dione derivatives **3a**–**3c** and sodium dithiocarbamate derivatives **6a**–**6e** in DMF at 50 °C.

### *Pharmacology*

*ChE Inhibitory Activity.* The phthalimide-dithiocarbamate hybrids **7a**–**7o** were screened against AChE/BuChE by the Ellman's method.[18] Inhibitory activity of these compounds was compared to standard drugs rivastigmine and donepezil (*Table 1*). As can be seen in *Table 1*, compounds **7b** and **7g**–**7i** were potent

 

inhibitors against AChE and among them, **7g** was the most potent inhibitor ($IC_{50} = 4.6 \pm 0.18$ μM). This compound was 2.5-fold more active than rivastigmine ($IC_{50} = 11.07 \pm 0.01$ μM). Other synthesized compounds did not show any activity against AChE at 100 μM.

Based on the $IC_{50}$ values for BuChE, most of the title compounds exhibited satisfactory inhibitory activity against BuChE in the range of $8.8 \pm 0.24$–$30 \pm 0.46$ μM compared with rivastigmine ($IC_{50} = 7.72 \pm 0.02$ μM) and donepezil ($IC_{50} = 7.79 \pm 0.06$). Among them, compounds **7b**, **7c**, **7h**, and **7o** were found to be more potent inhibitors. Six compounds **7a**, **7d**, **7f**, **7k**, **7m**, and **7n** showed no activity against BuChE at 100 μM.

Structurally, the synthesized compounds are divided into two series: secondary amine derivatives **7a**–**7i** and tertiary amine derivatives **7j**–**7o**. In each series, the amine groups and length of the linker between phthalimide and dithiocarbamate moieties were altered to optimize the anti-ChE inhibitory activity.

The inhibitory activity of secondary amine derivatives **7a**–**7i** against AChE demonstrated that benzylpiperidine derivative **7g** with methylene linker showed the most potent activity. Replacement of the methylene linker to ethylene and propylene led to decreases of 2.5 and 6 fold inhibitory activity as observed in the compounds **7h** and **7i**, respectively. In this series, cyclohexane derivative **7b** with ethylene linker showed a moderate inhibitory activity against AChE while it analogs **7a** and **7c** with methylene and propylene linkers showed no activity against AChE. Moreover, phenyl derivatives **7d**–**7f** showed no anti-AChE activity. Our obtained results were also shown that tertiary amine derivatives **7j**–**7o** were not active against AChE.

In the term of BuChE inhibitory activity in secondary amine series **7a**–**7i**, benzylpiperidine derivative **7h** with ethylene linker showed most potent activity while its methylene and propylene analogs **7g** and **7i** showed moderate and no activity against BuChE, respectively. Interestingly, for cyclohexane derivatives **7a**–**7c** and phenyl derivatives **7d**–**7f**, similar to benzylpiperidine derivatives **7g**–**7i**, the most potent compounds were compounds containing ethylene linker (compounds **7b** and **7e**, respectively). In this regard, changing ethylene linker to propylene linker in compound **7b**, as in compound **7c**, slightly diminished the activity while replacement of ethylene linker with methylene linker, as in compound **7a**, led to loss of anti-BuChE activity. Moreover, for phenyl derivatives **7d**–**7f**, replacement of the ethylene linker to methylene and propylene linkers led to loss of inhibitory activity against BuChE (compound **7e** vs. compounds **7d** and **7f**).

For the tertiary amine derivatives **7j**–**7o**, phenylpiperazine derivative **7o** with propylene linker exhibited the highest inhibitory activity against BuChE. The rest phenylpiperazine derivatives **7j**–**7k** did not show any activity against BuChE. In this series, two piperidine derivatives **7j** and **7 l** with methylene and ethylene linkers showed moderate activity while their propylene analog **7k** was inactive against BuChE.

*Molecular Docking and Dynamic Studies*. Docking study was performed using by AutoDock 4.2 package to find the binding modes of the most potent compounds **7g** and **7h** in the active site of AChE and BuChE, respectively. For this purpose, the X-ray crystal structure of AChE (PDB code: 6O4 W) and BuChE (PDB code: 4BDS) were retrieved of RCSB protein data bank (http://www.rcsb.org/pdb/home/home.do).

The applied docking procedure reliability was validated by re-docking of standard inhibitors donepezil and tacrine over AChE and BuChE, respectively. The docked conformations corresponding to the lowest docking score were selected as the most possible binding modes. The root mean square deviation (RMSD) was calculated for each ligand to measure the docking prediction accuracy. The pose was counted optimal if its RMSD found to be less than 2 Å. The RMSD of the re-docked conformations of donepezil and tacrine over 6O4 W and 4BDS was 0.40 Å and 0.29 Å, respectively, which is considered as successfully docked.[19,20] As a result, the validity of docking parameters are reasonable in order to predict the related co-crystalized structures.

Docking of donepezil over AChE active site showed that the ring center of the benzyl and the indene moiety interacted with Trp86 and Trp286 *via* $\pi$–$\pi$ interactions, respectively. Also, the quaternary amine of piperidine ring interacts by two $\pi$-cation interactions with the ring center of Trp86 and Phe338, as well the indene carbonyl group forms H-bond interaction with the backbone N–H of Phe295 (2.3 Å) (*Figure 2a*)

Furthermore, docking of tacrine over BuChE showed the prominent role of Trp82 and His438 in stabilizing the ligand in the binding pocket by constructing $\pi$–$\pi$ and $\pi$-cation interactions with the aromatic part of acridine moiety and H-bond with the quaternary amine at the distance of 2.5 Å, respectively (*Figure 2b*).

In order to understand the criteria for rational designing of ChEs inhibitors, it is necessary to uncover the structural perturbations incurred by the most potent compounds over ChEs and the effect of these

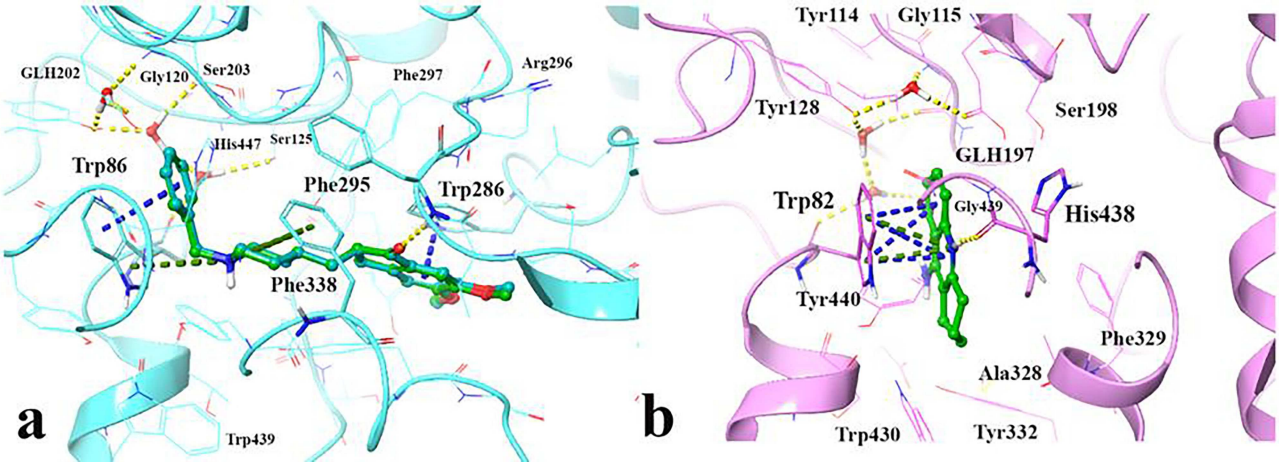


**Figure 2.** Close-up representation of binding interactions of the superposed docked (green) and co-crystalized donepezil and tacrine (cyan) over AChE (a) and BuChE (b), respectively, structural waters and their H-bond interaction render in stick.

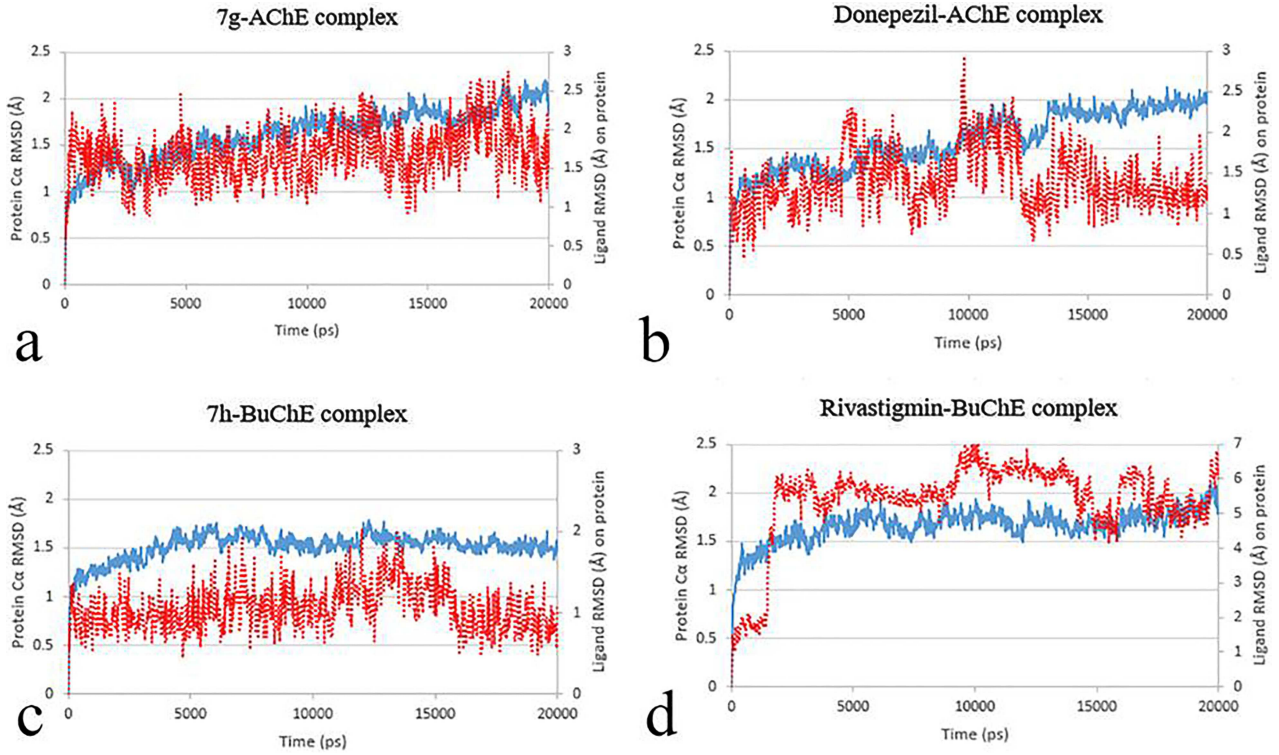


**Figure 3.** RMSD of ligand (red) and protein C$\alpha$ (blue) for **7g**-AChE (a), donepezil-AChE (b), **7h**-BuChE (c), and **7h**-BuChE (d) over 20 ns MD simulation time.

compounds on the active site environment. Here, the stability of protein-ligand complex is defined by RMSD of the protein's backbone from its initial to final conformation over 20 ns MD simulation time. The RMSD simulation showed that AChE complexed with **7g** and donepezil maintained an overall stability throughout the last 2 and 5 ns of MD time, respectively, with higher fluctuation stabilizing at an average of 2.2 Å for both systems (*Figure 3a* and *3b*), while the complex of rivastigmine and **7h** complexed with BuChE displayed longer equilibration time (about the last 15 ns) with lower fluctuations (*Figure 3c* and *3d*). The RMSD value of each protein-ligand complex indicates that the employed simulation time has been

 

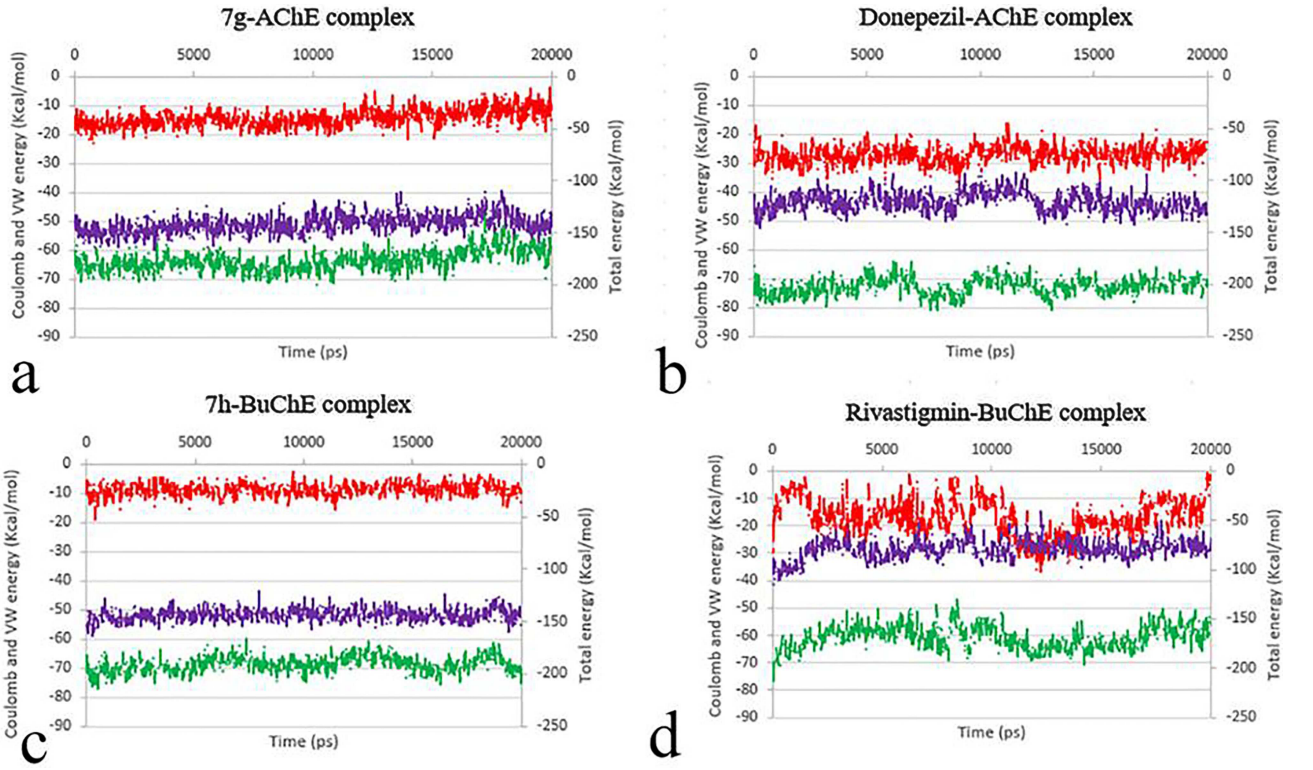


**Figure 4.** The variation of interaction energy of the compounds over the AChE and BuChE during 20 ns of MD simulation. Coulomb, Van der Waals (Vw), and total energy are in red, purple, and green, respectively.

enough to obtain an equilibrium structure over the simulation time. Thus, the structures at the MD equilibrium state used to investigate the structural specificity of the ligand-protein complexes.

Interaction energies were calculated in order to reveal ligand-protein stability of AChE/**7g**, donepezil or BuChE/**7h**, rivastigmine (*Figure 4*). The average total interaction energy for the compound **7g** over AChE was −10/−20 kcal/mol and for donepezil over AChE was −20/−30 kcal/mol. Comparing the total interaction energy obtained from MD for the **7g** with donepezil, it was observed that donepezil has more average total interaction energy (more stable) throughout 20 ns of simulation time as compared to that of **7g** (*Figure 4a* and *4b*). As the total energy of a system is the sum of coulomb and Van der Waals (Vw) energies, this difference originally is due to the more coulomb energy of donepezil over AChE than compound **7g**. According to the experimental assay, higher AChE inhibition activity of donepezil rather than **7g** may be related to the more stability and higher interaction energy of donepezil in comparison with compound **7g**. On the other hand, compound **7h** with higher Vw and total interaction energy than rivastigmine (*Figure 4c* and *4d*) show almost the same anti-BuChE activity which highlight the possibility of correlation between interaction and inhibitory activity.

*Figure 5a* and *5c* show the detailed ligand atom interactions that occurred more than 30.0% of the simulation and *Figure 5b* and *5d* represent protein–ligand contact bar occupancy during the 20 ns simulations for **7g** and donepezil. The interaction analysis suggests the piperidine $NH^+$ group in **7g** stabilized by $\pi$-cation interaction with Trp86 of catalytic anionic site (CAS) and Tyr341 at the peripheral anionic site (PAS), and form H-bond interaction with Tyr124 of PAS with high occupancy during the simulation time. In addition, dithiocarbamate moiety stabilized through water mediated H-bond interactions with Phe295 and Arg296 from the acyl-binding pocket of CAS. Furthermore, the acyl-binding pocket of CAS interacts with phthalimide moiety through Ser293 and Phe338 with H-bond and hydrophobic interactions (*Figure 5a*).

Comparison between the binding interactions of donepezil and **7g** with AChE revealed some differences between the two ligands interactions. The first Asp74 formed a strong and stable ionic interaction

 

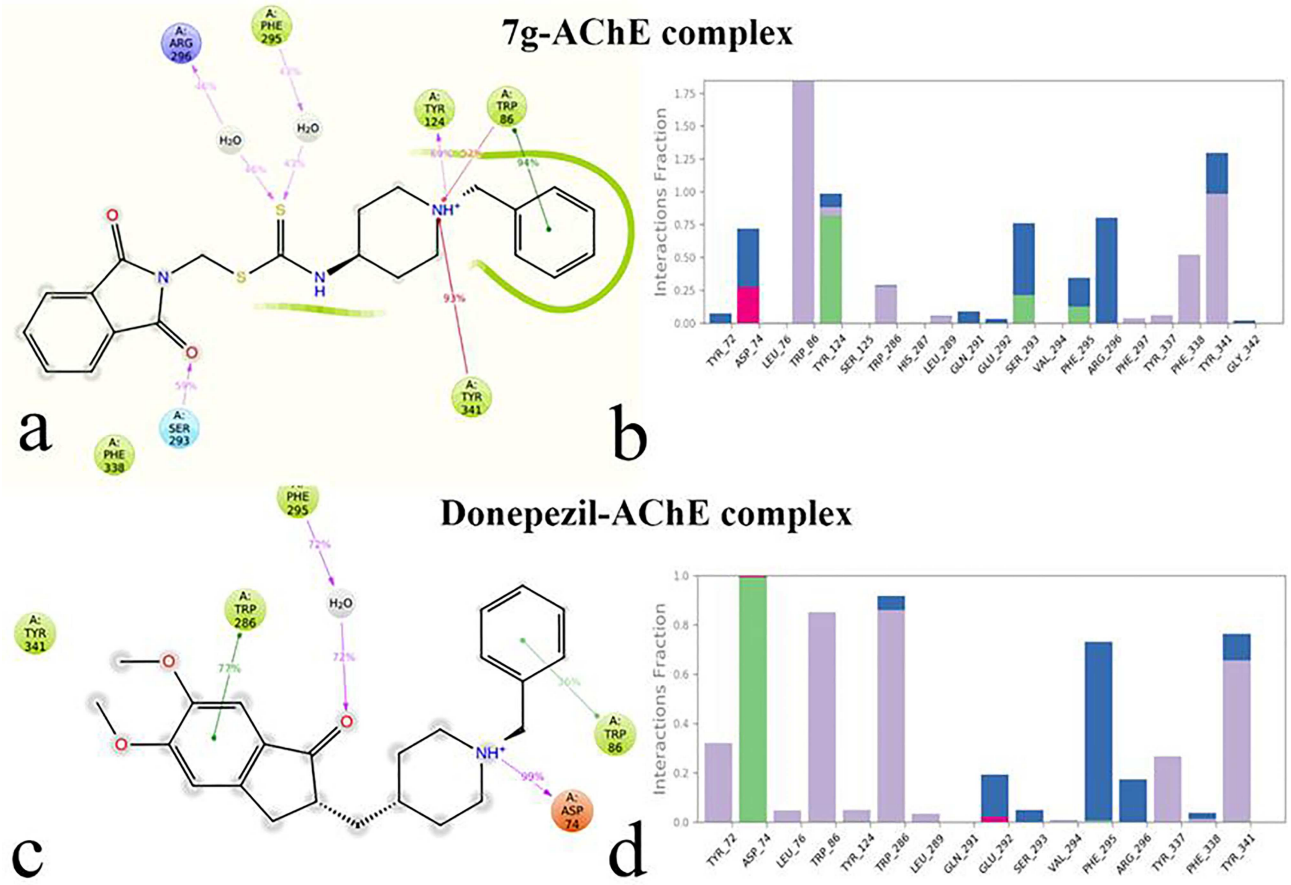


**Figure 5.** Detailed ligand atom interactions and protein-ligand contact bar analyzed at 20 ns simulations of **7g** (a, b) and donepezil (c, d) over AChE. Interactions that occur more than 30.0% of the simulation time are shown. H-bond, hydrophobic, ionic, and water bridge are in green, purple, pink, and blue, respectively.

between piperidine $NH^+$ group in donepezil with 99% time of simulation (*Figure 5c*, purple arrow), while the same $NH^+$ group in **7g** stabilized with Trp86, Tyr341, and Tyr124 as previously mentioned. Although these interactions have specific role in stabilizing **7g**, they are not as strong as ionic interaction participate in donepezil by the residue Asp74. Furthermore, by comparing *Figure 5b* and *5d* the outstanding contribution of Trp268 related to the PAS residues can be observed which stabilized the 1-oxoindane group of donepezil through $\pi-\pi$ stacking interactions with 77% time of simulation (*Figure 5c*, straight green lines). Consequently, donepezil is regarded as a more stable ligand in the binding pockets of the AChE, and subsequently more active compound to inhibit AChE than compound **7g**.

Regards to compound **7h**, the benzyl ring and the dithiocarbamate moiety established $\pi$-$\pi$ and H-bond interactions with Trp82 and Asn68 at PAS over the BuChE, respectively. Also, phthalimide moiety displayed $\pi$-$\pi$ interaction with Trp231 and Phe329 from the acyl-binding pocket of CAS. Furthermore, there is a strong ionic bridge between piperidine $NH^+$ group and Asp70 (*Figure 6a*, straight red and blue line) with 77% time of simulation that such strong interaction has been observed through donepezil and AChE (*Figure 5c*). The comparison between the binding interactions of rivastigmine and **7h** over BuChE represented that although the number of binding interactions with more that 30% occurrence among **7h** and BuChE are remarkably more than existing binding interactions between rivastigmine and BuChE, both of them show remarkable ionic interaction with Asp70 at the PAS (*Figure 6c*). Therefore, it is expected that **7h** to be as active as rivastigmine against BuChE. Our molecular dynamics study suggests that the persistent ionic interaction of ligand with the PAS residue Asp (Asp74 in AChE and Asp70 in BuChE) has a significant contribution for ChEs inhibition.

 

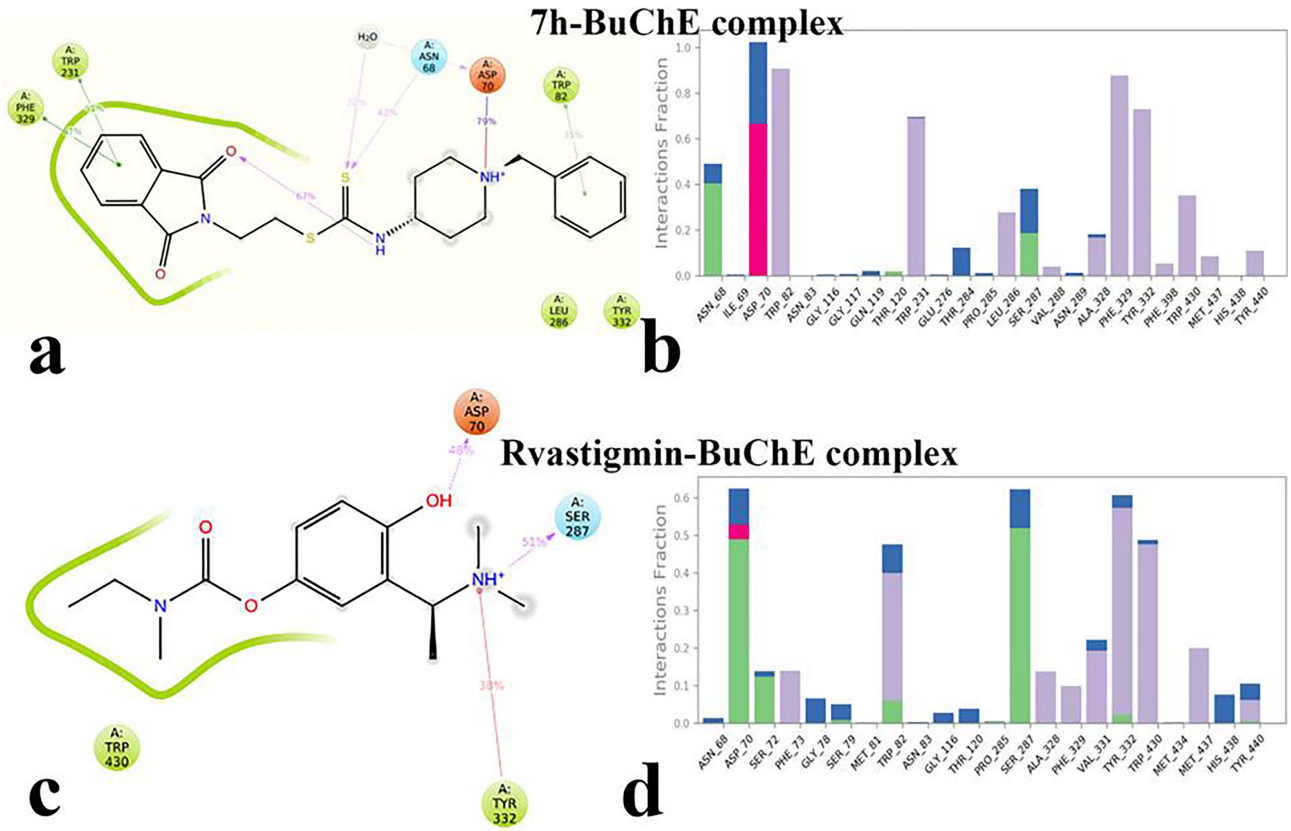


**Figure 6.** Detailed ligand atom interactions and protein-ligand contact bar analyzed at 20 ns simulations of **7h** (a, b) and rivastigmine (c, d) over BuChE. Interactions that occur more than 30.0 % of the simulation time are shown. H-bond, hydrophobic, ionic, and water bridge are in green, purple, pink, and blue, respectively.

For analyzing the fluctuation of ChEs residues over ligand binding interaction, the root mean square fluctuation (RMSF) was calculated from MD trajectories. Considering the RMSF plot of **7g** and **7h**, it was verified that they are in a good agreement with the corresponding plots of donepezil and rivastigmine, respectively (*Figure 7*). The residues that are bonded to the ligand were very stable along the simulations ($<$ 2 Å). In the case of BuChE, a larger fluctuation ($\geq$ 2 Å) was observed for the region relative to residues 281–283 which are located over the loop at the interface between the catalytic domain of BuChE and **7h**/rivastigmine binding site. This loop does not interact with the complexed ligand at the BuChE active site, so observing higher fluctuation is unavoidable. The regions showing high fluctuation in AChE-ligand complex are residues 259 to 264 and residues 493 to 498 that are located to the two side loops far from the active site and have high solvent exposure. RMSF results suggested that the complexes of compound **7g** and **7h** with the ChE enzyme were able to maintain their structural and the integrity during the simulations.

*Drug Likeliness Parameters*. The physicochemical properties and BBB penetration of the compounds **7g** and **7h** as the most potent compounds respectively against AChE and BuChE were predicted *in silico*. The physicochemical properties of these compounds and standard drugs rivastigmine and donepezil were obtained using MarvineSketch 5.8.3, ChemDrawUltra 12.0, and Autodock Tools (ver.1.5.4) to assess their compliance with the Lipinski's rule of five (a molecular weight (MW) $\leq$ 500, a number of H-bond acceptors (HBA) $\leq$ 10, a number of H-bond donors (HBD) $\leq$ 5, octanol-water partition coefficients (log P) $\leq$ 5, and a number of rotatable bonds (RBC) $\leq$ 10) and the Veber rule (polar surface area (tPSA) $\leq$ 140 Å$^2$).[21,22] As can be seen in *Table 2*, obtained data revealed that studied compounds follow the Lipinski's rule of five and the Veber rule. The BBB penetration of the compounds **7g**, **7h**, rivastigmine, and donepezil was predicted by the admetSAR server.[23] This software predicted that agents with SVM_MACCSFP BBB score $>$ 0.02 were

 

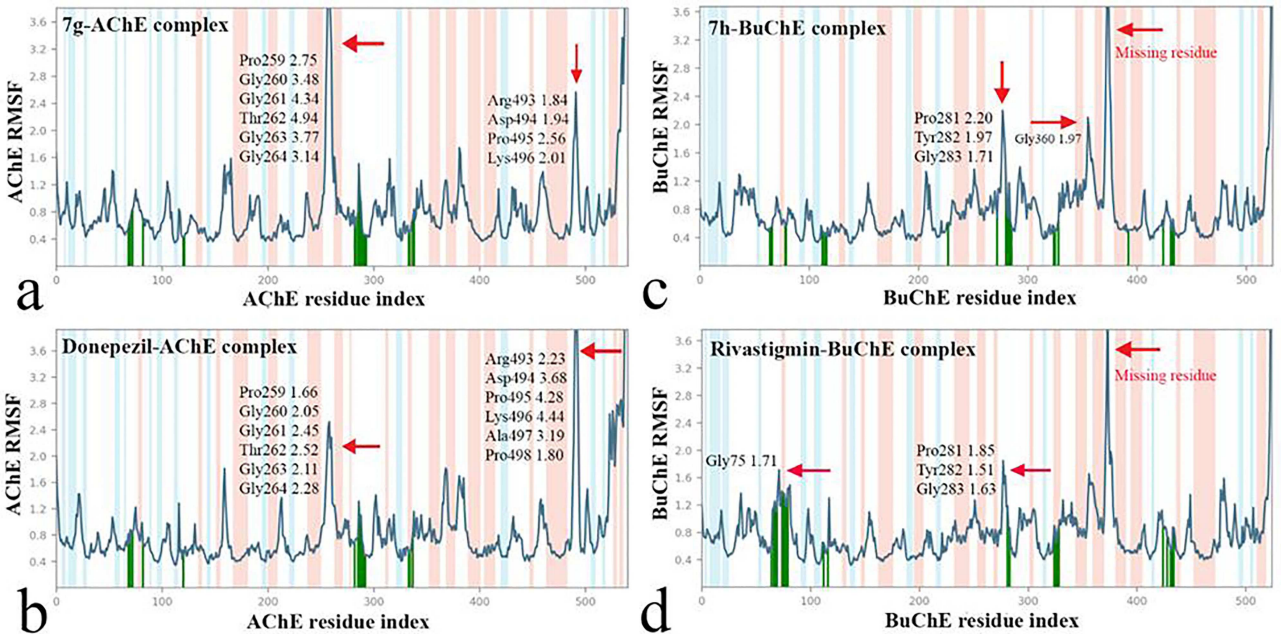


**Figure 7.** RMSF values of ChE enzyme from all different systems. **7g**-AChE (a), donepezil-AChE (b), **7h**-BuChE (c), rivastigmine-BuChE (d). Peaks indicate areas of the protein that fluctuated the most during the simulation. the background pink, blue and white strips represented the $\alpha$-helix and $\beta$ stands and the loop secondary structures of the enzymes, the ligand binding site represented in green bar at the bottom of the RMSF plot.

**Table 2.** Physicochemical properties and BBB penetration of the compounds **7g**, **7h**, Rivastigmine, and Donepezil.

| Entry | Rule | **7g** | **7h** | Rivastigmine | Donepezil |
|---|---|---|---|---|---|
| MW | $\leq$500 | 425 | 439 | 250.17 | 379.21 |
| HBA | $\leq$10 | 3 | 3 | 2 | 3 |
| HBD | $\leq$5 | 1 | 1 | 0 | 0 |
| LogP | $\leq$5 | 3.69 | 3.69 | 2.41 | 4.21 |
| RBC | $\leq$10 | 7 | 7 | 6 | 6 |
| Lipinski's violations | – | 0 | 0 | 0 | 0 |
| tPSA | $\leq$140 Å$^2$ | 52.65 | 52.65 | 32.78 | 38.77 |
| Veber violation | – | 0 | 0 | 0 | 0 |
| BBB score[a] | >0.02 | 0.056 | 0.053 | 0.042 | 0.103 |
| BBB penetration | – | + | + | + | + |

[a] SVM_MACCSFP BBB Score.

able to cross the BBB (*Table 2*). Obtained results revealed that studied synthesized compounds similar to standard drugs were able to cross the BBB.

*$\beta$-Secretase Inhibitory Activity.* One of the most important approaches for treatment of AD is inhibition of $\beta$-secretase (BACE-1) in order to prevent the formation of A$\beta$ plaques.[24] Thus, $\beta$-secretase inhibitory activity of compound 7g as the most active compound against AChE was obtained via a fluorescence resonance emission transfer (FRET) method. For this propose, the kit consisted of $\beta$-site amyloid precursor protein cleaving enzyme 1 (BACE-1) and Amyloid $\beta$-Protein Peptide (APP) based substrate (Rh-EVNLDAEFK-quencher) was applied and OM99-2 ($IC_{50}$ = 0.014 μM) was used as the reference agent. Obtained results showed that the compound 7g is a weak inhibitor against $\beta$-secretase (*Table 3*).

## Conclusions

In conclusion, we introduced a novel series of phthalimide-dithiocarbamate hybrids as new cholinesterase inhibitors. Two series of secondary amine

 

**Table 3.** $\beta$-Secretase inhibitory activity of compound **7g**.

| Compound | % Inhibition at 10 μM | % Inhibition at 50 μM | $IC_{50}$ [μM][a] |
|---|---|---|---|
| **7g** | 24 ± 12.7 | 39 ± 14.3 | ND |
| OM99-2 | – | – | 0.014 ± 0.003 |

[a] Mean ± S.E.; values are means of three independent experiments.

derivatives **7a**–**7i** and tertiary amine derivatives **7j**–**7o** were synthesized from appropriate dibromoalkanes, carbon disulfide, and various amine derivatives. The results of cholinesterase inhibitory activity revealed that secondary amine derivatives **7g** and **7h** were the most potent compounds against AChE and BuChE, respectively. Therefore, we made attempt to understand dynamics behavior and the detailed interactions of the compounds **7g** and **7h** against AChE and BuChE, respectively, and compare them with the FDA approved donepezil and rivastigmine. Our molecular dynamics study revealed that the complex of these compounds with the studied ChE was able to maintain their structural and integrity during the simulations based on RMSD, RMSF, and energy evaluation study. Furthermore, docking study revealed the persistent ionic interaction of the selected ligands with Asp in the PAS (Asp74 in AChE and Asp70 in BuChE) has a significant contribution for ChEs inhibition. *In silico* pharmacokinetic assay and BBB penetration prediction demonstrated that compounds **7g** and **7h** have satisfactory pharmacokinetics and BBB penetration as anti-Alzheimer drug candidates.

## Experimental Section

*Chemistry*

Melting points of phthalimide-dithiocarbamate derivatives **7a**–**7o** were measured with a Kofler hot stage apparatus and are uncorrected. $^{1}$H- and $^{13}$C-NMR spectra of the title compounds were recorded with Bruker FT-400, using TMS as an internal standard. IR spectra of these compounds were obtained with a Nicolet Magna FT-IR 550 spectrophotometer (KBr disks). MS were recorded with an Agilent Technology (HP) mass spectrometer operating at an ionization potential of 70 eV. Elemental analysis of the derivatives **7a**–**7o** was performed with an Elementar Analyses system GmbH VarioEL CHNS mode.

*General Procedure for the Preparation of 2-(Bromoalkyl)isoindoline-1,3-dione Derivatives* **3**

Potassium 1,3-dioxoisoindolin-2-ide (**1**; 1 mmol) and acetonitrile was put into a round-bottom flask and stirred at 60 °C. Then, appropriate dibromoalkanes **2a**–**2c** (2 mmol) were added dropwise to this mixture for 30 min. After that, the reaction mixture was stirred at 60 °C for 6 h. After completion of the reaction (monitored by TLC), acetonitrile was removed under vacuum. The obtained precipitate was filtered off and washed with diethyl ether to give pure compounds 2-(bromoalkyl)isoindoline-1,3-dione derivatives **3a**–**3c**.

*General Procedure for the Preparation of Sodium Dithiocarbamates* **6a**–**6e**

A mixture of different amines **5a**–**5e** (1 mmol) and 10% potassium hydroxide (1 mmol) in DMF (5 ml) was dissolved and cooled until 0 °C. Then, carbon disulfide (**4**; 1.5 mmol) was added dropwise to this mixture for 30 min. The reaction mixture was stirred and heated in 50 °C for 3 h. The reaction progress was monitored by TLC. After completion of the reaction, the mixture was cooled to room temperature and a mixture of water/ice was added and the obtained mixture was filtered to give sodium dithiocarbamate **6a**–**6e**.

*General Procedure for the Preparation of 2-(1,3-Dioxoisoindolin-2-yl)alkyl Piperidine-1-carbodithioates* **7a**–**7o**

A mixture of 2-(bromoalkyl)isoindoline-1,3-dione derivatives **3a**–**3c** (1 mmol) and sodium dithiocarbamates **6a**–**6e** (1 mmol) in DMF was stirred at 50 °C for 12 h. Then, the reaction mixture was allowed to cool at room temperature and poured into crushed ices, and subsequently, the pure white precipitates were filtered off. The pure products **7a**–**7o** were obtained by recrystallization from ethanol.

*Biological Evaluation*

*In Vitro AChE and BChE Inhibition Assay*. The inhibitory potency of the phthalimide-dithiocarbamate hybrids **7a**–**7o** on AChE and BuChE was evaluated using Ellman's method.[18] All the synthesized compounds were dissolved in 1 mL DMSO and 9 mL ethanol and then four different concentrations (56.3, 11.3, 2.2, and 0.45 μM per well) of each compound were tested to obtain the range of 20–80% enzyme inhibition for AChE/BuChE. The reaction mixture included 50 μL phosphate buffer (0.1 M, pH = 8.0), 125 μL of 0.1 M

DTNB, 25 μL of enzyme (2 U/mL of AChE (E.C. 3.1.1.7, Type V–S, lyophilized powder, from electric eel) or BuChE (E.C. 3.1.1.8, from equine serum), and 25 mL of inhibitor solution. The changing of the absorbance was measured at 412 nm for 2 min (30 s intervals) after addition of 10 μL substrate (acetylthiocholine iodide or butyrylthiocholine iodide, 0.15 M) to the reaction mixture by a multi-well plate reader (Gen5, Power wave xs2, BioTek, America). The $IC_{50}$ values were determined graphically from inhibition curves (log inhibitor concentration vs. percent of inhibition). All experiments were performed in 24-well plates on a Synergy HTX microplate reader in quadruplicates.

*Molecular Docking Study*

In order to find out the interactions mode of designed molecules over ChE enzyme, Maestro Molecular Modeling platform (version 11.5) by Schrödinger, LLC was performed.[25] Initially, the crystal structures of AChE and BuChE enzymes were retrieved from the Protein Data Bank (PDB: 6O4 W and 4BDS, respectively) (http://www.rcsb.org).[26,27] These pdb structures were selected based on criteria like; highest resolution (Å), being related to Homo sapiens specious, wild type with no modified residue, and the existence of co-crystalized ligand. As the prosthetic group and the co-factors are not directly involved in ChE inhibition, so they were totally removed before docking investigation. Except for the four structural waters molecule in the AChE and BuChE active site, which bridge the receptor important residues by way of H-bonds and conserve among other specious, the rest of the water molecules were removed from the enzymes crystallographic structures.[28] The 2D structures of the selected compounds were drawn in Marvin 15.10.12.0 program (http://www.chemaxon.com) and converted into pdb. The Protein Preparation Wizard and the LigPrep module were used to prepare protein and ligand structure properly.[29–31]

*Molecular Dynamic Simulation*

Molecular simulations of this study were performed using the Desmond v5.3 using Maestro interface (from Schrödinger 2018-4 suite).[32] We evaluated the stability of the best drug candidate from the experimental study; **7g** and **7h** over AChE and BuChE, respectively, and compared their perturbation with the standard inhibitor donepezil and rivastigmine, respectively.

Before the MD simulation, the appropriate pose for the compounds (**7g** and **7h**) over AChE and BuChE was determined by Glide docking protocol.[33,34] Glide application was used for docking investigations using the standard-precision followed by extra-precision method with flexible ligand sampling. Post-docking minimization was performed by applying strain correction terms. The best docking score poses were used for conducting MD simulation. In order to build system for md simulation, the protein-ligand complexes were solvated with SPC explicit water molecules and placed in the center of an orthorhombic box of appropriate size in the Periodic Boundary Condition. Sufficient counter-ions and a 0.15 M solution of NaCl were also utilized to neutralize the system and to simulate the real cellular ionic concentrations, respectively. The MD protocol involved minimization, pre-production, and finally production MD simulation steps. In the minimization procedure, the entire system was allowed to relax for 2500 steps by the steepest descent approach. Then, the temperature of the system was raised from 0 to 300 K with a small force constant on the enzyme in order to restrict any drastic changes. MD simulations were performed via NPT (constant number of atoms, constant pressure, i.e., 1.01325 bar and constant temperature, i.e., 300 K) ensemble. The Nose-Hoover chain method was used as the default thermostat with 1.0 ps interval and Martyna-Tobias-Klein as the default barostat with 2.0 ps interval by applying isotropic coupling style. Long-range electrostatic forces were calculated based on Particle-mesh-based Ewald approach with the he cut-off radius for coulombic forces set to 9.0 Å. Finally, this system was subjected to production MD simulations for 20 ns for each protein-ligand complex. During the simulation, every 1000 ps of the actual frame was stored. The dynamic behavior and structural changes of the systems were analyzed by the calculation of energy and the root mean square deviation (RMSD). Subsequently, the energy-minimized structure calculated from the equilibrated trajectory system was evaluated for investigation of each ligand-protein complex.

*In Silico Molecular Properties Prediction*

The HBA, HBD, and log P values of the compounds **7g**, **7h**, rivastigmine, and donepezil were calculated using the MarvineSketch 5.8.3. The tPSA and RBCs of these compounds were calculated using ChemDrawUltra 12.0 and Autodock Tools (ver.1.5.6), respectively. Prediction of BBB penetration of the test compounds

 

was performed by online BBB predictor (www.cbligand.org).

*BACE1 Enzymatic Assay*

$\beta$-Secretase inhibitory assay of the compound **7g** was performed exactly according to the manufacturer's instruction for BACE1 ($\beta$-Secretase) FRET Assay Kit (Invitrogen. http://tools.invitrogen.com/content/sfs/manuals/L0724.pdf).

## Acknowledgements

This research has been supported by a grant from the Research Council of Tehran University of Medical Sciences (Grant No. 97-01-108-3787).

## Author Contribution Statement

Mahmood Biglar, Bagher Larijani, and Roghieh Mirzazadeh contributed the reagents and materials, and analyzed the data. Saghi Sepehri and Maryam Mohammadi-Khanaposhtani performed the *in silico* studies. Mehdi Asadi and Mostafa Ebrahimi performed the synthesis of compounds. Hamid Nadri and Najmeh Edraki performed the biological assay. Massoud Amanlou and Mohammad Mahdavi conceived and designed the experiments.

## References

[1] K. P. Kepp, 'Alzheimer's disease due to loss of function: A new synthesis of the available data', *Prog. Neurobiol.* **2016**, *143*, 36–60.
[2] C. Patterson, 'The World Alzheimer Report 2018', 'The State of the Art of Dementia Research: New Frontiers', Alzheimer's Disease International (ADI), London, 2018.
[3] A. Kumar, A. Singh, 'A review on Alzheimer's disease pathophysiology and its management: an update', *Pharmacol. Rep.* **2015**, *67*, 195–203.
[4] M. Prior, R. Dargusch, J. L. Ehren, C. Chiruta, D. Schubert, 'The neurotrophic compound J147 reverses cognitive impairment in aged Alzheimer's disease mice', *Alzheimer's Res. Ther.* **2013**, *5*, 25.
[5] B. M. McGleenon, K. B. Dynan, A. P. Passmore, 'Acetylcholinesterase inhibitors in Alzheimer's disease', *Br. J. Clin. Pharmacol.* **1999**, *48*, 471.
[6] G. G. Osborn, A. V. Saunders, 'Current treatments for patients with Alzheimer Disease', *J. Am. Osteopath. Assoc.* **2010**, *110*, S16–S26.
[7] J. Kara, P. Suwanhom, C. Wattanapiromsakul, T. Nualnoi, J. Puripattanavong, P. Khongkow, V. S. Lee, A. Gaurav, L. Lomlim, 'Synthesis of 2-(2-oxo-2*H*-chromen-4-yl) acetamides as potent acetylcholinesterase inhibitors and molecular insights into binding interactions', *Arch. Pharm. Chem. Life Sci.* **2019**, e1800310.
[8] U. Sharma, P. Kumar, N. Kumar, B. Singh, 'Recent advances in the chemistry of phthalimide analogs and their therapeutic potential', *Mini-Rev. Med. Chem.* **2010**, *10*, 678–704.
[9] A. M. Alanazi, A. S. El-Azab, I. A. Al-Suwaidan, K. E. H. ElTahir, Y. A. Asiri, N. I. Abdel-Aziz, A. M. Alaa, 'Structure-based design of phthalimide derivatives as potential cyclooxygenase-2 (COX-2) inhibitors: anti-inflammatory and analgesic activities', *Eur. J. Med. Chem.* **2015**, *92*, 115–123.
[10] P. Ahuja, A. Husain, N. Siddiqui, 'Essential amino acid incorporated GABA-phthalimide derivatives: synthesis and anticonvulsant evaluation', *Med. Chem. Res.* **2014**, *23*, 4085–4098.
[11] S. P. Assis, T. G. Araújo, V. L. Sena, M. T. J. Catanho, M. N. Ramos, R. M. Srivastava, V. L. Lima, 'Synthesis, hypolipidemic, and anti-inflammatory activities of arylphthalimides', *Med. Chem. Res.* **2014**, *23*, 708–716.
[12] R. Antunes, H. Batista, R. M. Srivastava, G. Thomas, C. C. Araújo, R. L. Longo, H. Magalhães, M. B. Leão, A. C. Pavão, 'Synthesis, characterization and interaction mechanism of new oxadiazolo-phthalimides as peripheral analgesics', *J. Mol. Struct.* **2003**, *660*, 1–13.
[13] C. Pessoa, P. M. P. Ferreira, L. V. C. Lotufo, M. O. de Moraes, S. M. Cavalcanti, L. C. D. Coêlho, M. Z. Hernandes, A. C. L. Leite, C. A. De Simone, V. M. Costa, V. M. Souza, 'Discovery of phthalimides as immunomodulatory and antitumor drug prototypes', *ChemMedChem: Chem. Enabl. Drug Discov.* **2010**, *5*, 523–528.
[14] N. Guzior, M. Bajda, M. Skrok, K. Kurpiewska, K. Lewiński, B. Brus, A. Pišlar, J. Kos, S. Gobec, B. Malawska, 'Development of multifunctional, heterodimeric isoindoline-1,3-dione derivatives as cholinesterase and $\beta$-amyloid aggregation inhibitors with neuroprotective properties', *Eur. J. Med. Chem.* **2015**, *92*, 738–749.
[15] Z. Sang, K. Wang, H. Wang, L. Yu, H. Wang, Q. Ma, M. Ye, X. Han, W. Liu, 'Design, synthesis and biological evaluation of phthalimide-alkylamine derivatives as balanced multifunctional cholinesterase and monoamine oxidase-B inhibitors for the treatment of Alzheimer's disease', *Bioorg. Med. Chem. Lett.* **2017**, *27*, 5053–5059.
[16] N. Jiang, Q. Huang, J. Liu, N. Liang, Q. Li, Q. Li, S. S. Xie, 'Design, synthesis and biological evaluation of new coumarin-dithiocarbamate hybrids as multifunctional agents for the treatment of Alzheimer's disease', *Eur. J. Med. Chem.* **2018**, *146*, 287–298.
[17] N. Jiang, J. Ding, J. Liu, X. Sun, Z. Zhang, Z. Mo, X. Li, H. Yin, W. Tang, S. S. Xie, 'Novel chromanone-dithiocarbamate hybrids as multifunctional AChE inhibitors with $\beta$-amyloid anti-aggregation properties for the treatment of Alzheimer's disease', *Bioorg. Chem.* **2019**, 103027.
[18] G. L. Ellman, K. D. Courtney, V. Andres Jr., R. M. Featherstone, 'A new and rapid colorimetric determination of acetylcholinesterase activity', *Biochem. Pharmacol.* **1961**, 88–95.
[19] J. A. Erickson, M. Jalaie, D. H. Robertson, R. A. Lewis, M. Vieth, 'Lessons in molecular recognition: the effects of

 

ligand and protein flexibility on molecular docking accuracy', *J. Med. Chem.* **2004**, *47*, 45–55.
[20] J. W. M. Nissink, C. Murray, M. Hartshorn, M. L. Verdonk, J. C. Cole, R. Taylor, 'New test set for validating predictions of protein-ligand interaction', *Proteins Struct. Funct. Genet.* **2002**, *49*, 457–471.
[21] C. A. Lipinski, 'Drug-like properties and the causes of poor solubility and poor permeability', *J. Pharmacol. Toxicol. Methods* **2000**, *44*, 235–249.
[22] D. F. Veber, S. R. Johnson, H. Y. Cheng, B. R. Smith, K. W. Ward, K. D. Kopple, 'Molecular properties that influence the oral bioavailability of drug candidates', *J. Med. Chem.* **2002**, *45*, 2615–2623.
[23] F. Cheng, W. Li, Y. Zhou, J. Shen, Z. Wu, G. Liu, P. W. Lee, Y. Tang, 'AdmetSAR: a comprehensive source and free tool for evaluating chemical ADMET properties', *J. Chem. Inf. Model.* **2012**, *52*, 3099–3105.
[24] R. Yan, R. Vassar, 'Targeting the $\beta$ secretase BACE1 for Alzheimer's disease therapy', *Lancet Neurol.* **2014**, *13*, 319–329.
[25] L. L. C. Schrodinger, 'Schrödinger Suite 2012 Induced Fit Docking protocol', Glide version 5.8, New York, NY, Schrodinger, LLC, 2009.
[26] O. Gerlits, K. Y. Ho, X. Cheng, D. Blumenthal, P. Taylor, A. Kovalevsky, Z. A. Radic, 'New crystal form of human acetylcholinesterase for exploratory room-temperature crystallography studies', *Chem.-Biol. Interact.* **2019**, *309*, 108698–108698.
[27] F. Nachon, E. Carletti, C. Ronco, M. Trovaslet, Y. Nicolet, L. Jean, P. Renard, 'Crystal Structures of Human Cholinesterases in Complex with Huprine W and Tacrine: Elements of Specificity for Anti-Alzheimer's Drugs Targeting Acetyl- and Butyrylcholinesterase', *Biochem. J.* **2013**, *453*, 393–399.
[28] T. Rosenberry, X. Brazzolotto, I. Macdonald, M. Wandhammer, M. Trovaslet-Leroy, S. Darvesh, F. Nachon, 'Comparison of the binding of reversible inhibitors to human butyrylcholinesterase and acetylcholinesterase: A crystallographic, kinetic and calorimetric study', *Molecules* **2017**, *22*, 2098.
[29] Marvin 15.10.12.0, 2015, ChemAxon http://www.chemaxon.com.
[30] Schrödinger Release 2018–4: Schrödinger Release 2018–4 Protein Preparation Wizard; Epik, Schrödinger, LLC, New York, NY, 2016; Impact, Schrödinger, LLC, New York, NY, 2016; Prime, Schrödinger, LLC, New York, NY, 2019.
[31] Schrödinger Release 2018–4: LigPrep, Schrödinger, LLC, New York, NY, 2018.
[32] Schrödinger Release 2018–4: Desmond Molecular Dynamics System, D. E. Shaw Research, New York, NY, 2019. Maestro-Desmond Interoperability Tools, Schrödinger, New York, NY, 2018.
[33] T. A. Halgren, R. B. Murphy, R. A. Friesner, H. S. Beard, L. L. Frye, W. T. Pollard, J. L. Banks, 'Glide: A New Approach for Rapid, Accurate Docking and Scoring. 2. Enrichment Factors in Database Screening', *J. Med. Chem.* **2004**, *47*, 1750–1759
[34] R. A. Friesner, J. L. Banks, R. B. Murphy, T. A. Halgren, J. J. Klicic, D. T. Mainz, M. P. Repasky, E. H. Knoll, D. E. Shaw, M. Shelley, J. K. Perry, P. Francis, P. S. Shenkin, 'Glide: A New Approach for Rapid, Accurate Docking and Scoring. 1. Method and Assessment of Docking Accuracy', *J. Med. Chem.* **2004**, *47*, 1739–1749.

*Received July 4, 2019*
*Accepted September 9, 2019*

 